Line Spectrum of Tungsten Ions at Low Ionization Stages in Large Helical Device in Wavelength Range of 300 - 2400 Å Measured Using 20 cm Normal Incidence VUV Spectrometers*)

Tetsutarou OISHI[1,2)], Shigeru MORITA[1,2)], Xianli HUANG[2)], Hongming ZHANG[2)], Motoshi GOTO[1,2)] and the LHD Experiment Group[1)]

[1)]*National Institute for Fusion Science, 322-6 Oroshi-cho, Toki 509-5292, Japan*

[2)]*Department of Fusion Science, Graduate University for Advanced Studies, 322-6 Oroshi-cho, Toki 509-5292, Japan*

(Received 26 November 2014 / Accepted 22 February 2015)

Vacuum ultraviolet (VUV) spectra of emissions released from tungsten ions at lower ionization stages were measured in the Large Helical Device (LHD) using three 20 cm normal incidence spectrometers in the wavelength range of 300 to 2400 Å. Tungsten ions were introduced in the LHD plasma by injecting a pellet consisting of a small piece of tungsten metal and polyethylene tube. The VUV spectroscopy revealed that WVI 639.683 Å, 677.722 Å, and 639.683×2 Å lines were useful lines for monitoring tungsten ion behaviors because they had large intensities and were isolated from other intrinsic impurity lines.

Keywords: vacuum ultraviolet, plasma spectroscopy, magnetically confined fusion, impurity transport, tungsten

DOI: 10.1585/pfr.10.3402031

1. Introduction

Behavior of multiply charged ions in fusion plasmas represented by tungsten ions has attracted attention because tungsten is regarded as a leading candidate material for the plasma facing components in ITER and future fusion reactors [1–3]. Considering transport processes of tungsten impurity in ITER, first, neutral tungsten atoms are released from the divertor plates, then tungsten ions at lower ionization stages are transported in the edge plasmas, and finally tungsten ions at higher ionization stages are distributed in the confinement region. In H-mode plasmas in tungsten-wall machines, it has been frequently observed that highly ionized tungsten ions are accumulated in the plasma core region with a high concentration, which results in a large radiation loss and a deterioration of the energy confinement property [4,5]. Therefore, diagnostics for tungsten impurity ions in magnetically-confined high-temperature plasmas have been intensively conducted, such as visible spectroscopy for neutral tungsten atoms in the wavelength range around 4000 Å and extreme ultraviolet (EUV) spectroscopy for highly-ionized tungsten ions in the wavelength range around 15 - 70 Å [6]. Moreover, measurement of tungsten ions at lower ionization stages started recently using vacuum ultraviolet (VUV) spectroscopy in the wavelength range around 500 - 2200 Å because it is necessary for accurate evaluation of tungsten influx and comprehensive understanding of the tungsten impurity transport in high temperature plasmas [7].

Based on these results, spectral identification is attempted in this study for tungsten lines in a broad wavelength range of 300 - 2400 Å measured using three 20 cm normal incidence VUV spectrometers which have been utilized to monitor spectra of impurity emissions for all specified shots in the Large Helical Device (LHD). VUV spectroscopic techniques utilizing compact spectrometers with relatively poor wavelength resolution have been widely applied to tokamak plasmas to monitor impurity spectra over a broad wavelength range [8]. Although the diagnostic method in this study is ordinary, the measurement of tungsten impurities in LHD is important to understand the transport in helical plasmas. Furthermore, exploration of tungsten lines at low ionization stages which can be measured by the survey spectrometers routinely will contribute to spectroscopic studies on ITER edge plasmas.

2. Experimental Setup

Tungsten ions are introduced in the LHD plasma by injecting a polyethylene pellet containing a small piece of tungsten metal. LHD has the major/minor radii of 3.6/0.64 m in the standard configuration with maximum plasma volume of 30 m^3 and toroidal magnetic field of 3 T. The coil system consists of a set of two continuous superconducting helical coils with poloidal pitch number of 2 and toroidal pitch number of 10 and three pairs of superconducting poloidal coils [9]. The tungsten impurity pellet consists of a small piece of tungsten wire covered by a polyethylene tube. The length and diameter of tungsten

author's e-mail: oishi@LHD.nifs.ac.jp

*) This article is based on the presentation at the 24th International Toki Conference (ITC24).

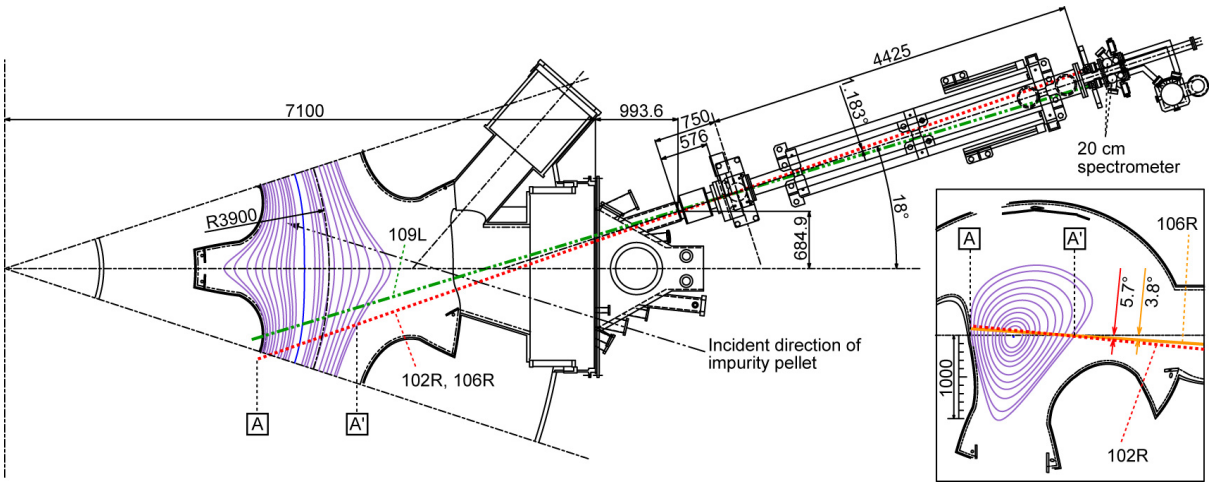

Fig. 1 Schematic drawing of VUV spectroscopy system using 20 cm normal incidence VUV spectrometers in LHD. Top view of magnetic surfaces (R_{ax} = 3.6 m), optical axis of three spectrometers (102R, 106R, and 109L), incident direction of impurity pellet, and a plasma cross section including optical axis of two spectrometers (102R and 106R) are shown together.

wire is 0.6 mm and 0.15 mm, respectively. The polyethylene tube has a dimension of 0.6 mm in length, 0.6 mm in outer diameter, and 0.3 mm in inner diameter [10]. The pellet is accelerated by pressurized He gas of 10 - 20 atm. The pellet injection direction is located on the midplane of the plasma having a 12° angle from the normal to the toroidal magnetic axis [11].

Figure 1 illustrates a schematic drawing of the VUV spectroscopy system using 20 cm normal incidence VUV spectrometers in LHD. Top view of magnetic surfaces (position of the magnetic axis R_{ax} = 3.6 m), optical axis of three spectrometers named "102R", "106R", and "109L", incident direction of impurity pellet, and a plasma cross section including optical axis of two spectrometers (102R and 106R) are shown together. The optical axis of 102R has an angle of 5.7° against the midplane, and those of 106R and 109L are 3.8°. Each spectrometer covered a wavelength range, $\Delta\lambda$, of 300 - 1050 Å with a wavelength dispersion, dλ/dx, of 0.85 Å/pixel (109L), $\Delta\lambda$ of 1000 - 1850 Å with dλ/dx of 0.88 Å/pixel (106R), and $\Delta\lambda$ of 1550 - 2400 Å with dλ/dx of 0.88 Å/pixel (102R), respectively, in a single discharge. Back-illuminated CCD detectors (Andor model DO420-BN: 1024 × 256 pixels, pixel size 26 × 26 μm^2) were placed at the positions of the exit slits of the spectrometers. A time resolution of 5 ms was applied to measure temporal evolution of the spectra. It is important that these three spectrometers are routinely operated in LHD, therefore we can obtain spectroscopic data in $\Delta\lambda$ of 300 - 2400 Å for all specified shots.

3. Measurement of Tungsten Emission Lines

Figure 2 shows the VUV spectra including tungsten emissions of WVI 605.926 Å, 639.683 Å, and 677.722 Å lines. Figure 2 (a) shows a spectrum measured using a 3 m normal incidence spectrometer with dλ/dx of 0.037 Å/pixel [12]. Spectra of three shots measured by scanning the wavelength shot by shot to cover a wavelength range of 600 - 700 Å are shown together. Three bright lines of 5d-6p transitions of tungsten WVI 605.926 Å, 639.683 Å, and 677.722 Å have been already identified in the previous study [7]. Figures 2 (b-d) show spectra measured using three 20 cm normal incidence spectrometers. Wavelength ranges of 600 - 700 Å, 1200 - 1400 Å, and 1800 - 2100 Å are enlarged to investigate above three tungsten lines and their second and third order emissions. Spectra measured before the pellet injections are also shown together. As shown in Figs. 2 (b) and (c), WVI 639.683 Å and 677.722 Å lines, and their second order lines were isolated from other intrinsic impurity lines even under observation with the wavelength resolution of a 20 cm VUV spectrometer while WVI 605.926 Å was blended with intrinsic OIV lines. Third orders of WVI lines were not found, as shown in Fig. 2 (d).

Figure 3 shows temporal evolutions of plasma parameters and line intensities of tungsten WVI lines. Line intensities were evaluated from the areas of the spectral peaks obtained by Gaussian fittings. Figure 3 (a) shows the central electron density, n_{e0}, and central electron temperature, T_{e0}. Figure 3 (b) shows the edge electron density, $n_e(a_{99})$, and edge electron temperature, $T_e(a_{99})$ at the effective minor radius of $r_{eff} = a_{99}$, which is defined as radius of 99 % of electron stored energy inside of the radius [13]. After the pellet injection, $n_e(a_{99})$ increases and $T_e(a_{99})$ drops rapidly followed by an increase of n_{e0} and a drop of T_{e0}. Figure 3 (c) shows the line intensity of tungsten WVI 677.722 Å line measured using a 3 m VUV spectrometer with a time resolution of 50 ms. Figures 3 (d-g) show the line intensities of WVI 639.683 Å, 677.722 Å, 639.683 × 2 Å, and 677.722 × 2 Å, respectively. Behaviors of the line intensities in Figs. 3 (c-f) are similar to each

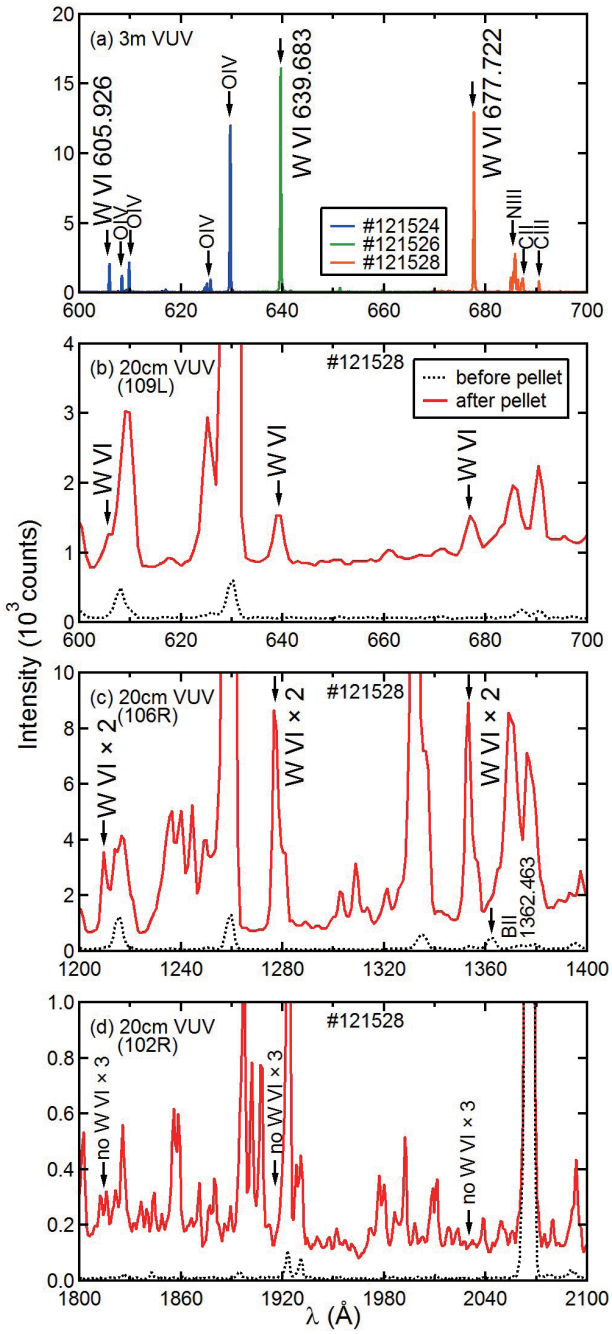

Fig. 2 VUV spectra including tungsten emissions of WVI 605.926 Å, 639.683 Å, and 677.722 Å lines. (a) spectrum measured using a 3 m normal incidence spectrometer for three shots with scanning the wavelength for shot by shot to cover a wavelength range of 600 - 700 Å. (b-d) spectra measured using three 20 cm normal incidence spectrometers. Wavelength ranges of 600 - 700 Å, 1200 - 1400 Å, and 1800 - 2100 Å are enlarged. Spectra measured before the pellet injection are also shown together.

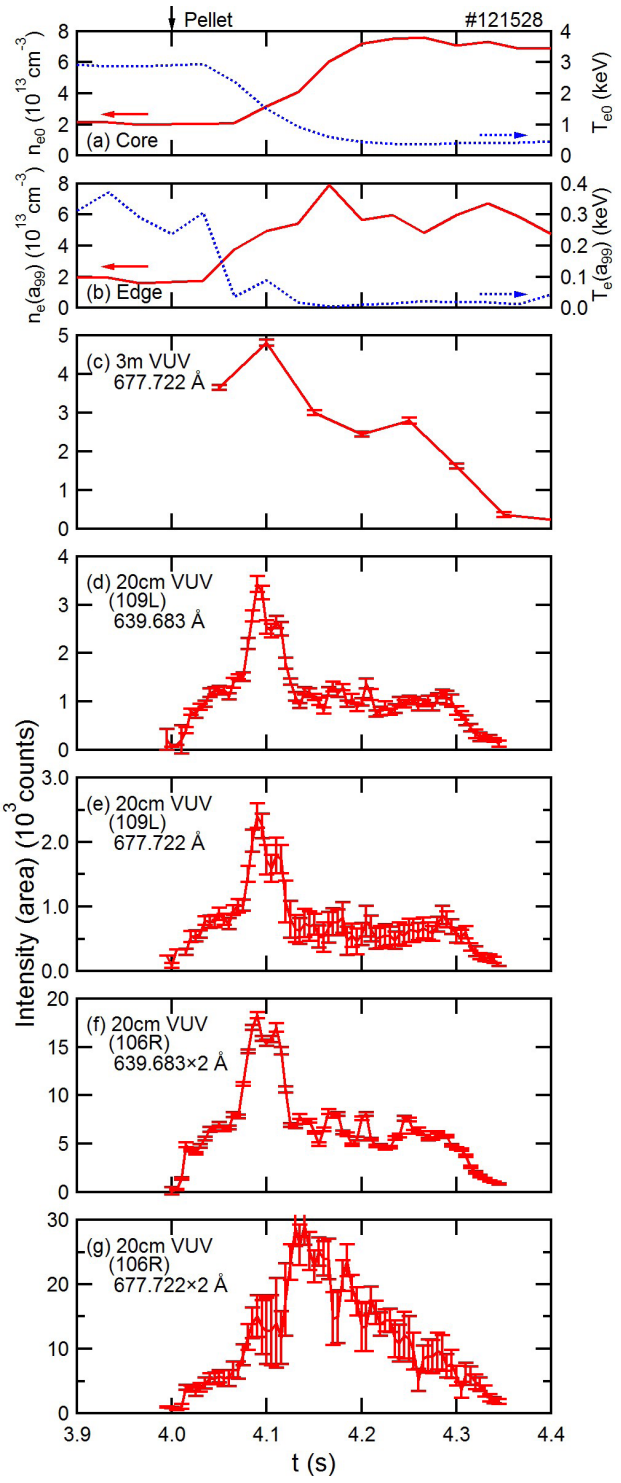

Fig. 3 Temporal evolutions of (a) central and (b) edge electron density and temperature, (c) line intensity of tungsten WVI 677.722 Å measured using a 3 m normal incidence VUV spectrometer, (d-g) line intensities of WVI 639.683 Å, 677.722 Å, 639.683 × 2 Å, and 677.722 × 2 Å measured using 20 cm normal incidence VUV spectrometers. Tungsten pellet is injected at 4.0 s.

other: they have a maximum value at 4.1 s, stay in almost constant value in 4.15 - 4.30 s, and disappear to 4.35 s. On the other hand, intensity of 677.722 × 2 Å in Fig. 3 (g) exhibited a different behavior because it is blended with neighboring boron BII 1362.463 Å which is identified as an intrinsic impurity, as shown in "before pellet" spectrum in Fig. 2 (c). Therefore, this 677.722 × 2 Å line is considered to be less appropriate as an indicator monitoring the tungsten behavior. The temporal evolutions of WVI inten-

sity shown in Figs. 3 (c-f) are correlated with the temporal evolution of $T_e(a_{99})$ having a local maximum value at 4.1 s shown in Fig. 3 (b). It suggests that W^{5+} ions are localized at the plasma edge region and the change of $T_e(a_{99})$ around the ionization potential of W^{5+} ions of 64.8 eV might have effects on the ionization and recombination processes. On the other hand, a decay of WVI intensity starting at 4.28 s is not explained well at present because atomic processes and transport phenomena should be taken into account for the detailed transport analysis, which will be investigated in future studies.

4. Summary

VUV spectroscopy using three 20 cm normal incidence spectrometers has been applied to measure VUV lines from tungsten ions at lower ionization stages. Each spectrometer covers $\Delta\lambda$ = 300 - 1050 Å with $d\lambda/dx$ = 0.85 Å/pixel (109L), $\Delta\lambda$ = 1000 - 1850 Å with $d\lambda/dx$ = 0.88 Å/pixel (106R), and $\Delta\lambda$ = 1550 - 2400 Å with $d\lambda/dx$ = 0.88 Å/pixel (102R), respectively, in a single discharge. These three spectrometers are routinely operated in LHD to provide spectroscopic data in $\Delta\lambda$ of 300 - 2400 Å for all discharges. Several tungsten lines have been observed after the tungsten pellet was injected into the LHD plasma. WVI 639.683 Å, 677.722 Å, and 639.683 × 2 Å lines had large intensities and were isolated from other intrinsic impurity lines. These lines will be useful not only for the spectroscopic studies of tungsten ions in LHD but also for ITER and other tungsten-wall machines.

Acknowledgements

The authors thank all the members of the LHD Experiment Group for their cooperation with the LHD operation. This work was partially conducted under the LHD project financial support (NIFS13ULPP010). This work was also supported by Grant-in-Aid for Young Scientists (B) 26800282 and partially supported by the JSPS-NRF-NSFC A3 Foresight Program in the Field of Plasma Physics (NSFC: No.11261140328, NRF: No.2012K2A2A6000443).

[1] ITER Physics Basis Editors *et al.*, Nucl. Fusion **39**, 2137 (1999).
[2] R. Neu *et al.*, Nucl. Fusion **45**, 209 (2005).
[3] J. Roth *et al.*, Plasma Phys. Control. Fusion **50**, 103001 (2008).
[4] R. Neu *et al.*, J. Nucl. Mater. **313-316**, 116 (2003).
[5] C. Angioni *et al.*, Nucl. Fusion **54**, 083028 (2014).
[6] S. Morita *et al.*, AIP Conf. Proc. **1545**, 143 (2013), Proceedings of ICAMDATA-2012, Gaithersburg, 30 Sept.–4 Oct. 2012.
[7] T. Oishi *et al.*, Rev. Sci. Instrum. **85**, 11E415 (2014).
[8] R.J. Fonck *et al.*, Appl. Opt. **21**, 2115 (1982).
[9] H. Yamada for the LHD Experiment Group, Nucl. Fusion **51**, 094021 (2011).
[10] X.L. Huang *et al.*, Rev. Sci. Instrum. **85**, 11E818 (2014).
[11] H. Nozato *et al.*, Rev. Sci. Instrum. **74**, 2032 (2003).
[12] T. Oishi *et al.*, Appl. Opt. **53**, 6900 (2014).
[13] K.Y. Watanabe *et al.*, Plasma Phys. Control. Fusion **49**, 605 (2007).